Designation: F2450 – 10

Standard Guide for Assessing Microstructure of Polymeric Scaffolds for Use in Tissue-Engineered Medical Products[1]

This standard is issued under the fixed designation F2450; the number immediately following the designation indicates the year of original adoption or, in the case of revision, the year of last revision. A number in parentheses indicates the year of last reapproval. A superscript epsilon (ε) indicates an editorial change since the last revision or reapproval.

1. Scope

1.1 This guide covers an overview of test methods that may be used to obtain information relating to the dimensions of pores, the pore size distribution, the degree of porosity, interconnectivity, and measures of permeability for porous materials used as polymeric scaffolds in the development and manufacture of tissue-engineered medical products (TEMPs). This information is key to optimizing the structure for a particular application, developing robust manufacturing routes, and providing reliable quality control data.

1.2 The values stated in SI units are to be regarded as standard. No other units of measurement are included in this standard.

1.3 *This guide does not purport to address all of the safety concerns, if any, associated with its use. It is the responsibility of the user of this standard to establish appropriate safety and health practices and to determine the applicability of regulatory limitations prior to use.*

2. Referenced Documents

2.1 *ASTM Standards:*[2]

D2873 Test Method for Interior Porosity of Poly(Vinyl Chloride) (PVC) Resins by Mercury Intrusion Porosimetry (Withdrawn 2003)[3]

D4404 Test Method for Determination of Pore Volume and Pore Volume Distribution of Soil and Rock by Mercury Intrusion Porosimetry

E128 Test Method for Maximum Pore Diameter and Permeability of Rigid Porous Filters for Laboratory Use

E1294 Test Method for Pore Size Characteristics of Membrane Filters Using Automated Liquid Porosimeter (Withdrawn 2008)[3]

E1441 Guide for Computed Tomography (CT) Imaging

F316 Test Methods for Pore Size Characteristics of Membrane Filters by Bubble Point and Mean Flow Pore Test

F2150 Guide for Characterization and Testing of Biomaterial Scaffolds Used in Tissue-Engineered Medical Products

F2603 Guide for Interpreting Images of Polymeric Tissue Scaffolds

3. Terminology

3.1 *Definitions:*

3.1.1 *bioactive agent, n*—any molecular component in, on, or within the interstices of a device that is intended to elicit a desired tissue or cell response.

3.1.1.1 *Discussion*—Growth factors and antibiotics are typical examples of bioactive agents. Device structural components or degradation byproducts that evoke limited localized bioactivity are not bioactive agents.

3.1.2 *blind (end)-pore, n*—a pore that is in contact with an exposed internal or external surface through a single orifice smaller than the pore's depth.

3.1.3 *closed cell, n*—a void isolated within a solid, lacking any connectivity with an external surface. Synonym: *closed pore*

3.1.4 *hydrogel, n*—a water-based open network of polymer chains that are cross-linked either chemically or through crystalline junctions or by specific ionic interactions.

3.1.5 *macropore/macroporosity* (life sciences) , *n*—a structure (including void spaces) sized to allow substantially unrestricted passage of chemicals, biomolecules, viruses, bacteria, and mammalian cells. In implants with interconnecting pores, macroporosity provides dimensions that allow for ready tissue penetration and microvascularization after implantation. Includes materials that contain voids with the potential to be observable to the naked eye (>100 μm).

3.1.6 *micropore/microporosity* (life sciences) , *n*—a structure (including void spaces) sized to allow substantially unrestricted passage of chemicals, biomolecules, and viruses while sized to control or moderate the passage of bacteria, mammalian cells, and/or tissue. Includes materials with typical pore

[1] This guide is under the jurisdiction of ASTM Committee F04 on Medical and Surgical Materials and Devices and is the direct responsibility of Subcommittee F04.42 on Biomaterials and Biomolecules for TEMPs.

Current edition approved March 1, 2010. Published April 2010. Originally approved in 2004. Last previous edition approved in 2009 as F2450 – 09. DOI: 10.1520/F2450-10.

[2] For referenced ASTM standards, visit the ASTM website, www.astm.org, or contact ASTM Customer Service at service@astm.org. For *Annual Book of ASTM Standards* volume information, refer to the standard's Document Summary page on the ASTM website.

[3] The last approved version of this historical standard is referenced on www.astm.org.

sizes of greater than 0.1 μm (100 nm) and less than about 100 μm (100 000 nm), with a common microporous context encompassing the range of 20 μm or less for the filtration of cells ranging from bacteria to common mammalian cells and above 30 μm for the ingrowth of tissue. Objects in this size range typically can be observed by conventional light microscopy.

3.1.7 *nanopore/nanoporosity* (life sciences), *n*—a structure inclusive of void spaces sized to control or moderate the passage of chemicals, biomolecules, and viruses while sized to substantially exclude most bacteria and all mammalian cells. Includes materials with typical pore sizes of less than 100 nm (0.1 μm), with common nanoporous context in the range of ~20 nm or less for the filtration of viruses.

3.1.8 *permeability, n*—a measure of fluid, particle, or gas flow through an open pore structure.

3.1.9 *polymer, n*—a long chain molecule composed of monomers including both natural and synthetic materials. Examples include collagen and polycaprolactone.

3.1.10 *pore, n*—a fluid (liquid or gas) filled externally connecting channel, void, or open space within an otherwise solid or gelatinous material (for example, textile meshes composed of many or single fibers (textile based scaffolds), open cell foams, (hydrogels)). Synonyms: *open-pore, through-pore*.

3.1.11 *porogen, n*—a material used to create pores within an inherently solid material.

3.1.11.1 *Discussion*—For example, a polymer dissolved in an organic solvent is poured over a water-soluble powder. After evaporation of the solvent, the porogen is leached out, usually by water, to leave a porous structure. The percentage of porogen needs to be high enough to ensure that all the pores are interconnected.

3.1.12 *porometry, n*—the determination of the distribution of open pore diameters relative to the direction of fluid flow by the displacement of a non-volatile wetting fluid as a function of pressure.

3.1.13 *porosimetry, n*—the determination of the pore volume and pore size distribution through the use of a non-wetting liquid (typically mercury) intrusion into a porous material as a function of pressure.

3.1.14 *porosity, n*—property of a solid which contains an inherent or induced network of channels and open spaces. Porosity can be determined by measuring the ratio of pore (void) volume to the apparent (total) volume of a porous material and is commonly expressed as a percentage.

3.1.15 *scaffold, n*—a support, delivery vehicle, or matrix for facilitating the migration, binding, or transport of cells or bioactive molecules used to replace, repair, or regenerate tissues.

3.1.16 *through-pores, n*—an inherent or induced network of voids or channels that permit flow of fluid (liquid or gas) from one side of the structure to the other.

3.1.17 *tortuosity, n*—a measure of the mean free path length of through-pores relative to the sample thickness. Alternative definition: The squared ratio of the mean free path to the minimum possible path length.

4. Summary of Guide

4.1 The microstructure, surface chemistry, and surface morphology of polymer-based tissue scaffolds plays a key role in encouraging cell adhesion, migration, growth, and proliferation. The intention of this guide is to provide a compendium of techniques for characterizing this microstructure. The breadth of the techniques described reflects the practical difficulties of quantifying pore sizes and pore size distributions over length scales ranging from nanometres to sub-millimetres and the porosity of materials that differ widely in terms of their mechanical properties.

4.2 These microstructural data when used in conjunction with other characterization methods, for example, chemical analysis of the polymer (to determine parameters such as the molecular weight and its distribution), will aid in the optimization of scaffolds for tissue-engineered medical products (TEMPs). Adequate characterization is also critical to ensure the batch-to-batch consistency of scaffolds; either to assess base materials supplied by different suppliers or to develop robust manufacturing procedures for commercial production.

4.3 Application of the techniques described in this guide will not guarantee that the scaffold will perform the functions for which it is being developed but they may help to identify the reasons for success or failure.

4.4 This guide does not suggest that all listed tests be conducted. The choice of technique will depend on the information that is required and on the scaffold's physical properties; for example, mercury porosimetry will not yield meaningful data if used to characterize soft materials that deform during the test and cannot be used for hydrated scaffolds.

4.5 Table 1 provides guidance for users of this guide by providing a brief overview of the applicability of a range of different measurement techniques that can be used to physically characterize tissue scaffolds. This list of techniques is not definitive.

5. Significance and Use

5.1 The ability to culture functional tissue to repair damaged or diseased tissues within the body offers a viable alternative to xenografts or heterografts. Using the patient's own cells to produce the new tissue offers significant benefits by limiting rejection by the immune system. Typically, cells harvested from the intended recipient are cultured *in vitro* using a temporary housing or scaffold. The microstructure of the scaffold, that is, its porosity, the mean size, and size distribution of pores and their interconnectivity is critical for cell migration, growth and proliferation (Appendix X1). Optimizing the design of tissue scaffolds is a complex task, given the range of available materials, different manufacturing routes, and processing conditions. All of these factors can, and will, affect the surface texture, surface chemistry, and microstructure of the resultant scaffolds. Factors that may or may not be significant variables depend on the characteristics of a given

TABLE 1 A Guide to the Physical Characterization of Tissue Scaffolds

Generic Technique	Information Available	Section
Microscopy	Pore shape, size and size distribution; porosity.	6.1 (Electron microscopy) 6.2 (Optical microscopy) 6.2.3 (Confocal microscopy) 6.2.4 (Optical coherence tomography) 6.2.5 (Optical coherence microscopy)
X-Ray micro-computed Tomography (MicroCT)	Pore shape, size and size distribution; porosity.	6.3
Magnetic Resonance Imaging	Pore shape, size and size distribution; porosity.	6.4
Measurement of density	Porosity, pore volume	7.2
Porosimetry	Porosity, total pore surface area, pore diameter, pore size distribution	7.3
Porometry	Median pore diameter (assuming cylindrical geometry), through-pore size distribution	7.4
Diffusion of markers	Permeability	8.2
NMR	Pore size and distribution	7.5

cell type at any given time (that is, changes in cell behavior due to the number of passages, mechanical stimulation, and culture conditions).

5.2 Tissue scaffolds are typically assessed using an overall value for scaffold porosity and a range of pore sizes, though the distribution of sizes is rarely quantified. Published mean pore sizes and distributions are usually obtained from electron microscopy images and quoted in the micrometer range. Tissue scaffolds are generally complex structures that are not easily interpreted in terms of pore shape and size, especially in three dimensions. Therefore, it is difficult to quantifiably assess the batch-to-batch variance in microstructure or to make a systematic investigation of the role that the mean pore size and pore size distribution has on influencing cell behavior based solely on electron micrographs (Tomlins et al, (**1**)).[4]

5.2.1 Fig. 1 gives an indication of potential techniques that can be used to characterize the structure of porous tissue scaffolds and the length scale that they can measure. Clearly a

[4] The boldface numbers in parentheses refer to the list of references at the end of this standard.

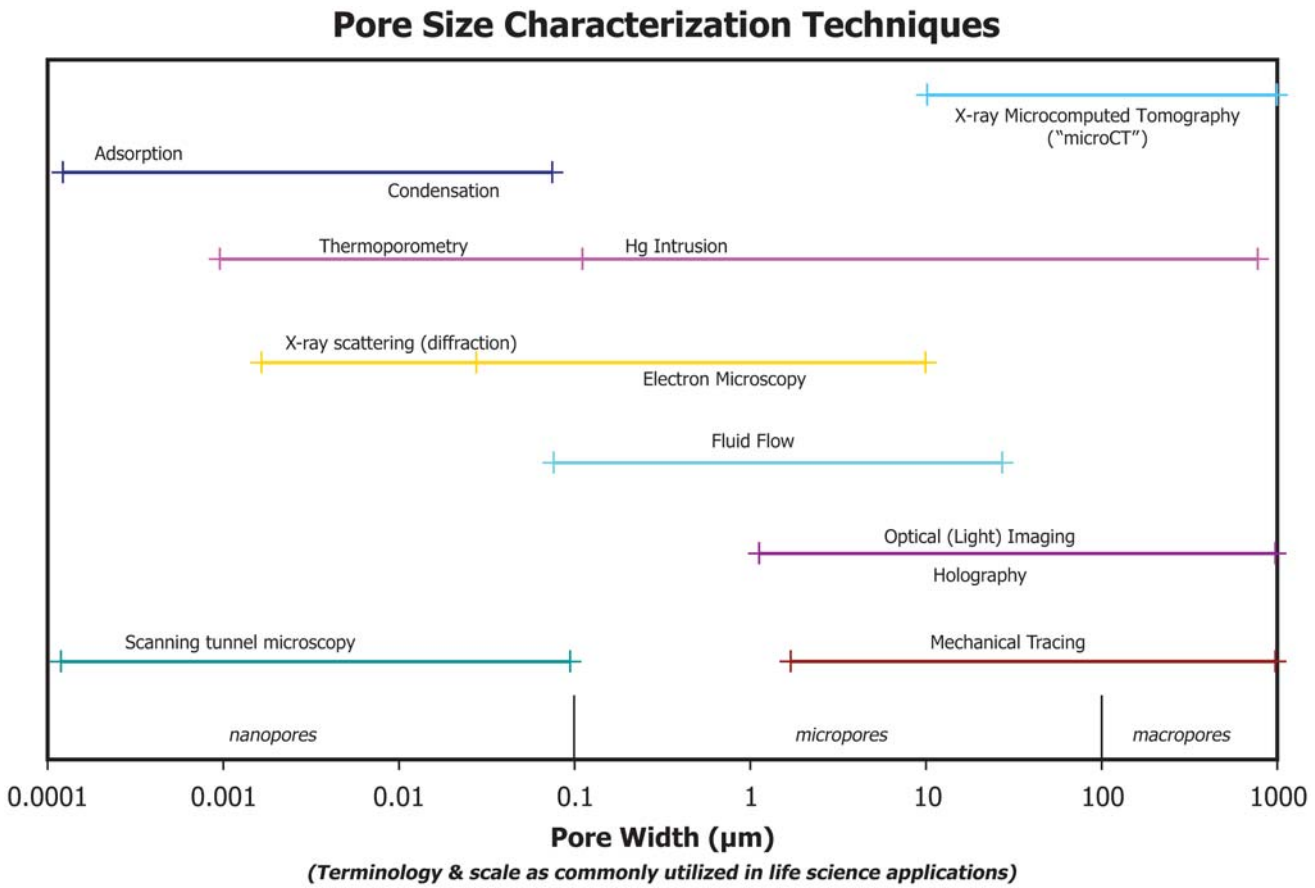

FIG. 1 A Range of Techniques is Required to Fully Characterize Porous Materials
(Note—Figure redrawn from Meyer (**2**).)

range of techniques must be utilized if the scaffold is to be characterized in detail.

5.2.2 The classification and terminology of pore sizes, such as those given in Table 2, has yet to be standardized, with definitions of terms varying widely (as much as three orders of magnitude) between differing applications and industries. Both Table 2 and the supporting detailed discussion included within Appendix X2 describe differences that exist between IUPAC (International Union of Pure and Applied Chemistry) definitions and the common terminology currently utilized within most life science applications, which include both implant and tissue engineering applications.

5.2.2.1 Since the literature contains many other terms for defining pores (Perret et al (**3**)), it is recommended that the terms used by authors to describe pores be defined in order to avoid potential confusion. Additionally, since any of the definitions in Table 2 can shift, dependending on the pore size determination method (see Table 1 and Fig. 1), an accompanying statement describing the utilized assessment technique is essential.

5.2.3 All the techniques listed in Table 1 have limitations for assessing complex porous structures. Fig. 2a and Fig. 2b show a through- and a blind-end pore respectively. Porometry measurements (see 7.4) are only sensitive to the narrowest point along a variable diameter through-pore and therefore can give a lower measure of the pore diameter than other investigative techniques, such as scanning electron microscope (SEM), which may sample at a different point along the pore. The physical basis of porometry depends on the passage of gas through the material. Therefore, the technique is not sensitive to blind-end or closed pores. Therefore, estimates of porosity based on porometry data will be different from those obtained from, for example, porosimetry (see 7.3), which is sensitive to both through- and blind-pores or density determinations that can also account for through-, blind-end, *and* closed pores. The significance of these differences will depend on factors such as the percentage of the different pore types and their dimensions. Further research will enable improved guidance to be developed.

5.2.4 Polymer scaffolds range from mechanically rigid structures to soft hydrogels. The methods currently used to manufacture these structures include, but are not limited to:

5.2.4.1 Casting a polymer, dissolved in an organic solvent, over a water-soluble particulate porogen, followed by leaching.

5.2.4.2 Melt mixing of immiscible polymers followed by leaching of the water-soluble component.

5.2.4.3 Dissolution of supercritical carbon dioxide under pressure into an effectively molten polymer, a phenomenon attributed to the dramatic reduction in the glass transition temperature which occurs, followed by a reduction in pressure that leads to the formation of gas bubbles and solidification.

5.2.4.4 Controlled deposition of molten polymer to produce a well-defined three-dimensional lattice.

5.2.4.5 The manufacture of three-dimensional fibrous weaves, knits, or non-woven structures.

5.2.4.6 Chemical or ionic cross-linking of a polymeric matrix.

5.2.5 Considerations have been given to the limitations of these methods in Appendix X1.

5.2.6 This guide focuses on the specific area of characterization of polymer-based porous scaffolds and is an extension of an earlier ASTM guide, Guide F2150.

6. Imaging

6.1 *Electron Microscopy*—Both transmission and scanning electron microscopy can be used to image intact or fractured surfaces or sections cut from tissue scaffolds. The resultant images can be interpreted using image analysis software packages to generate data concerning the shape of pores within the scaffold, their mean size, and their distribution. Estimates of both permeability and tortuosity can be made from three-dimensional virtual images generated from transmission electron microscopic images of serially sectioned samples.

6.1.1 There is likely to be a high degree of uncertainty in the reliability of quantitative data derived from electron microscopic examination of soft or especially highly hydrated soft polymer-based scaffolds due to the presence of artifacts created during sample preparation. Highly hydrated scaffolds need to be freeze-dried before examination under vacuum in a conventional scanning electron microscope (SEM). This process, if carried out in liquid nitrogen, usually results in a significant amount of ice damage due to the relatively slow cooling rates that are encountered due to the thin layer of insulating nitrogen gas that forms around the sample as it is frozen. Freezing samples in slush nitrogen can reduce ice damage by enabling faster cooling rates, apparently by reducing the thickness of the insulating gas layer.

6.1.2 The relatively new technique of cryogenic SEM may also be used to reduce artifacts. In this technique, a rapidly frozen specimen can be fractured whilst frozen within the cryo-SEM unit and sputter coated with gold-palladium after allowing some of the ice to sublime away. The amount of sublimation that occurs can be controlled through exposure time. With this technique, any freeze-drying of the sample is

TABLE 2 Comparison of Pore Size Nomenclature

Descriptor	IUPAC Definitions	Definitions for Life Science Applications
	For: chemical (for example, solid catalysts); metallurgy; geology (for example, zeolites) applications	*For: tissue engineering; medical implants; diagnostic or biological filtration applications*
Nanopore/nanoporosity	Not utilized	0.002 to 0.1 μm (2 to 100 nm)
Micropore/microporosity	<2 nm (<20 Å)	0.1 to 100 μm (typically defined 0.1 to 20 μm)
Mesopore	2 to 50 nm (20 to 500 Å)	Not utilized
Macropore/macroporosity	>50 nm (>500 Å)	>100 μm
Capillaries	Meyer, et al. (**2**)	Not utilized
Macrocapillaries	Meyer, et al. (**2**)	Not utilized

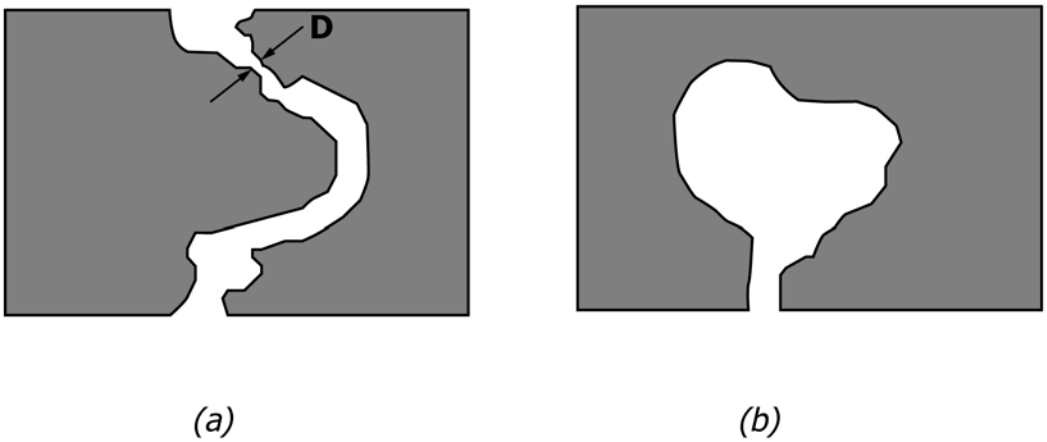

FIG. 2 A *through-pore* showing a variation of pore diameter, *D* (*a*); and an example of a *blind-pore* (*b*).

minimized. Experimentally validating the results obtained from this technique to ensure that they are artifact-free is difficult.

6.1.3 Polymer-based scaffolds often lack sufficient electron density to provide suitable levels of contrast; this can be overcome by staining using a high electron density material such as osmium tetroxide that has a high affinity for carbon-carbon double bonds.

6.1.4 Most polymer-based scaffolds can be mounted in epoxy resin using standard procedures and subsequently sectioned for serial examination in the transmission electron microscope. This method is less appropriate for investigating hydrogels that can dehydrate. However, this concern can be partially mitigated by gradual dehydration of the scaffold by using a series of alcohol solutions before embedding in resin. However, this procedure tends to reduce the size of the water-filled pores within the sample. Thus, the quantifiable pore size data subsequently obtained are of value when comparing microstructures between different samples. However, the results are less useful for characterizing expected *in vivo* microstructure due to sample distortion.

6.2 *Optical Microscopy-Based Methods:*

6.2.1 Optical methods can be utilized, providing sufficient contrast exists between the structure and surrounding media to enable surface features to be studied in a minimally prepared or natural state (that is, the specimen does not need to be stained or sectioned.) The disadvantage of this approach is that penetration of light into the sample can be limited, particularly for porous matrices, due to scattering. In practice, this limits the use of confocal microscopy and optical coherence tomography to depths that are typically less than 0.5 mm.

6.2.2 *Optical (Light) Microscopy*—Images of the surfaces of tissue scaffolds can be obtained using an optical microscope. Differential focus can used to collect images at different depths within semi-transparent specimens. These deep view images can be used to track the path of interconnected pores within the sample.

6.2.3 *Confocal Microscopy*—Substantial improvements in the quality of 'optically' sectioned samples can be made by either exploiting the natural fluorescent properties that the scaffold may have or by using a fluorescent stain such as fluorescein. Confocal microscopy can capture well-resolved images at different depths because of its shallow depth of field and elimination of out-of-focus light. A laser is usually used as a point light source in preference to a conventional lamp and in most modern instruments, several lasers are used. This capability is used to improve contrast within the image and to excite stains that bind to different structural elements and fluoresce at different wavelengths. Laser scanning confocal microscopy (LSCM) can be utilized in reflection or transmission modes. The size of the pinhole and the numerical aperture of the objective primarily determine the resolution in the thickness or axial direction. Generally, smaller holes give better resolution but at the expense of reduced intensity.

6.2.3.1 Some work on scaffold characterization using laser scanning confocal microscopy (LSCM) has been reported (Tjia and Moghe, (**4**), Birla and Matthew (**5**)).

6.2.4 *Optical Coherence Tomography*—Optical coherence tomography is a reflectance optical imaging technique that uses interferometric rejection of out-of-plane scattering of photons rather than a pinhole as in LSCM to determine axial resolution. Briefly, optical coherence tomography uses a low coherence source with a bandwidth of anywhere from 30 to 200 nm and an interferometer, usually of Michelson type, that generates profiles of back-reflected light for any one transverse position. For a complete description of optical coherence tomography and its applications, see Ref (**6**). An analogous technique is ultrasound A-scanning. In the Michelson configuration, the material is the fixed arm of the interferometer rather than a mirror. A low numerical aperture lens is used to achieve a large axial sampling volume and reflections from heterogeneities within the sample are mapped as a function of depth for any one position. Like LSCM, transverse resolution is determined by geometric optics. Unlike LSCM, axial resolution is inversely proportional to the bandwidth of the source, and a typical value for axial resolution is 10 mm.

6.2.4.1 The advantage of optical coherence tomography is that it is highly sensitive, typically 90 dB. Optical coherence tomography has been extensively used to image the human retina (Hee et al (**7**)), skin and blood vessels (Barton et al (**8**)), and the functioning circulatory systems of small live animals (Boppart et al (**9**)) with excellent clarity. In the late 1990s, the

potential for optical coherence tomography in the area of materials science was first seen. The first published optical coherence tomography images of a tissue-engineering scaffold were of a hydrogel and demonstrated the depth to which images can be obtained (McDonough et al (**10**)). The depth of field of the image is limited by scattering from the pores and any crystallites that are present. It can vary from approximately 100 μm to several millimetres depending on the difference in refractive index between the material and its surroundings, the level of porosity, and the pore size distribution. The penetration depth can be improved by filling the pores with a fluid of similar refractive index to the scaffold material. In practice, this is usually a substitution of water for air or oil for water. This procedure can result in additional problems due to poor wetting and trapped air. Optical coherence tomography images of porous materials tend to be noisy due to multiply scattered photons that contribute to the signal. A related technique, optical coherence microscopy, overcomes the issues related to the fidelity of imaging tissue-engineering scaffolds.

6.2.5 *Optical Coherence Microscopy*—Optical coherence microscopy is a combination of optical coherence tomography and confocal microscopy. Optical coherence microscopy is highly suited for imaging of optically opaque materials such as tissue-engineering scaffolds because it can attain axial and transverse resolution on the order of a micrometer and still maintain high background rejection. The confocal enhancement is done in the usual manner by the addition of a high numerical aperture objective and a pinhole, which is usually the open aperture of the sample arm fiber. For more information on optical coherence microscopy, see Ref (**6**). The key to the technique is the axial point spread functions (PSF) of the confocal and coherence techniques. For the confocal component, the Lorentzian axial PSF results in a finite collection efficiency even far out of the focus plane, and this limits its use in highly scattering media such as TEMPs. For the coherence component, the Gaussian PSF drops off far from the focal plane much more rapidly than that of confocal microscopy. Hence, the confocal component contributes to the high resolution near the focus and the coherence component contributes to the high background rejection, two qualities needed for effective imaging of TEMPs (Dunkers et al (**11**)).

6.3 *X-Ray Micro-computed Tomography (MicroCT)*—X-rays can be used to generate three-dimensional images of tissue scaffolds from which information on pore size and shape, porosity, and interconnectivity can be obtained. The principle of the method is to position the scaffold between an X-ray source and a detector. The sample is rotated and the X-ray attenuation is recorded at a number of different angles. These data can then be analyzed using reconstruction algorithms to produce an image of a two-dimensional slice through the scaffold. A full three-dimensional image can be generated from a series of two-dimensional slices obtained at different heights within the sample. Typical resolution of such an image is around 5 to 10 μm, but instruments that can resolve 50 nm are now commercially available. The success of the technique relies on there being sufficient contrast, that is, differences in electron density between the solid material and a fluid (typically air or water) within the pores.

6.3.1 The technique does not suffer from the same penetration depth limitations that optical tomographic methods suffer from, providing a more complete picture of the scaffold structure. Further information can be found in Guide E1441. The non-destructive approach has been used to investigate the structure of bone and other materials (Muller et al, (**12**), Muller et al, (**13**)) to validate the design of bone scaffolds (Van Oosterwijck et al, (**14**)) and to investigate polymeric scaffolds (Maspero et al (**15**), Lin et al (**16**)).

6.4 *Magnetic Resonance Imaging*—Many polymers contain magnetic resonance (MR) active nuclei (for example, 1H, 13C), but the relaxation times of nuclei on the polymer backbone are too short for routine imaging applications. Thus, to study the three-dimensional morphology of polymeric scaffolds, the pore space must be filled with a fluid, which is visible in a magnetic resonance imaging (MRI) experiment. The ideal fluid must contain MR active nuclei, which are naturally abundant, have a high receptivity, and have a well-resolved nuclear magnetic resonance (NMR) spectrum of narrow lines. Moreover, it needs to have a low viscosity to infiltrate the pore space and must have appropriate relaxation properties to provide a large signal, after the application of the imaging gradients. Fortunately, immersion in water will suffice for most polymeric scaffolds.

6.4.1 The theoretical limit in spatial resolution for MRI experiments is typically the distance (~10 μm) a water molecule diffuses during the time it takes to acquire the MRI signal. Thus, polymeric scaffolds with large pores (50 to 100 μm) can be spatially resolved with this technique. In MR images, the water-filled pores appear bright and the polymer mesh dark. High contrast images of the polymer mesh, after suitable image analysis, can be used to generate estimates of pore sizes and pore size distribution.

6.4.2 The porosity of scaffolds that have pores that are smaller than the resolution limit of the MRI technique can be estimated from the signal intensity of a water-saturated scaffold normalized to that of pure water. The normalized signal intensity reflects the volume fraction of water present within the polymer scaffold, if the polymer does not contribute to the measured signal. For hydrogels, a better estimate of the polymeric volume fraction can be derived from quantitative transverse relaxation maps. This approach is used to analyze the density of cross-links in hydrogels used as radiation dosimetry phantoms. For polymeric scaffolds with pore sizes comparable to the diameter of a cell (10 to 20 μm), MR images of the diffusion behaviour of the pore fluid can yield estimates of the pore size and size distribution. A limitation of this approach is the need to assume a geometric model to obtain structural information.

6.4.3 Other limitations of the MRI technique include its low spatial resolution and the necessity of a pore fluid to study the structure of the scaffold, which limits the technique to detecting only those pores that are fluid-filled. In practice, MRI will be unable to detect enclosed pores or those which either trap air (blind-end pores) or are difficult to wet out due to surface tension. The distribution of the pore fluid within the scaffold is

a potential measure of pore volume accessible to cells, although lack of signal in certain regions can be attributed to trapped air, solid polymer, or the presence of small diameter dry pores.

6.4.4 The advantage of the MRI technique is that polymeric scaffolds can be non-destructively investigated in three-dimensions, without the need for using stains or dyes. The scaffold does not need to be optically transparent and preparative techniques, which can alter the morphology of the polymeric scaffold, are not required. Additionally, this imaging modality can be used to monitor the distribution of cells and extracellular matrix proteins within the scaffold, both spatially and temporally. Furthermore, MRI can monitor the performance of a tissue scaffold *in vivo* as well as the biological response of the body to the scaffold material.

6.5 *Image Analysis*—Irrespective of which technique is used to image tissue scaffolds, it is imperative that due consideration is given to the quantitative determination of key structural parameters. Typically the porous regions within a digital image are selected using criteria set within the image analysis software. Basic measures of the structure including the number of pores, pore area (and hence pore volume), and total porosity are derived from these selected areas (for example, Scaglione et al, 2003 (**17**)). Further information regarding image capture, storage, and interpretation can be found in Guide F2603.

7. Physical Characterization

7.1 Measures of scaffold permeability can be used to assess the accessibility of the structure to migrating cells or to measure the ability of the structure to service the needs of an incumbent population of functional cells. All of the techniques described have their limitations and range of applicability for polymer-based scaffolds.

7.2 *Measurement of Density*—An estimate of the volume of pores within a scaffold can be obtained using the relationship between density and volume, providing the density of the material, ρ_s used to construct the scaffold is known. In this procedure, the volume of the scaffold, V_T is determined by measuring the sample dimensions. The mass of sample, m_s, is then measured. In some cases, it may be necessary to dry the sample to constant weight before weighing to ensure that any contributions from the water are removed. Clearly, this procedure should be followed for gels or materials that are known to have significant water content and for materials that are recognized to be hygroscopic. The volume of pores within the scaffold, V_P, is then calculated according to:

$$V_P = V_T - \frac{m_s}{\rho_s} \quad (1)$$

and the percentage porosity is $V_P / V_T \cdot 100$.

7.2.1 This measure of porosity provides an estimate of the total free space within a sample. While this quantity is useful, it has limited practical relevance, unless used with other more specific pore characterization measures, since it consists of contributions from the volumes of open pores, closed cells and blind-end pores.

7.2.2 Measurement of sample dimensions can be difficult for irregular geometries. In this case, the Archimedes principle can be used to determine the volume of the specimen from the volume of fluid displaced. It should be noted that the buoyancy method is not sensitive to enclosed pores and may not fully wet out through- or blind-end pores. Using this method with hydrophobic materials (for example, polycaprolactone), which are not easily wetted, can be experimentally challenging. However, such problems can be overcome by using small amounts of a wetting agent (for example, 1 % (volume) of ethanol) or by using an inert gas instead of a liquid as in helium pycnometry.

7.2.3 Estimates of the reliability of this measure have yet to be determined from the uncertainties in measuring the dimensions and mass of the sample and the density of the solid material, which for polymer-based materials, can be complicated due to cross-linking and crystallinity.

7.3 *Porosimetry (Liquid Intrusion)*—The volume of pores in a scaffold can be estimated by measuring the volume of a non-wetting fluid, typically mercury, required to fill all pores that have contact with an exposed surface. Test Methods D4404 and D2873 contain descriptions of this technique.

7.3.1 Mercury porosimetry can generate the following data: the total pore volume, the total pore surface area, the mean pore diameter, and the pore size distribution. Clearly, mercury intrusion will generate erroneous information for soft porous scaffolds because of the scaffold being distorted. Currently the relationship between scaffold distortion and scaffold wall stiffness is not known. The technique cannot be used to determine the porosity of hydrogels. Assessments of porosity using porosimetry often provide an underestimate of pore volume, as liquid will fill only those pores that are connected to exposed surfaces (that is, blind-end and through-pores). It should also be recognized that the pore size distribution generated by this technique is an equivalent structure because the theory (that is, the Washburn equation) assumes that pores are parallel sided. Thus pores that have a variable diameter along their length will contribute to a range of pore diameters that form the histogram of pore sizes.

7.4 *Porometry*—Gas flow porometry can be used to characterize some properties of through-pores. In this technique, increasing gas pressure is utilized to force a non-volatile wetting liquid from the interstices of the scaffold being characterized. Gas flow through both the dry and subsequently wet scaffold is measured as a function of the applied pressure. These data are then used to estimate the through-pore size distribution and median flow pore diameter (in mm) assuming cylindrical pore geometry. Details of the method can be found in Test Methods E128, E1294, and F316.

7.4.1 Through-pore diameters derived from this method represent the narrowest point along any given pore. Because of this limitation, the pore diameters determined by gas flow porometry appear to be smaller than those determined by other methods. This method does not provide information on closed or blind-end pores. Through-pores in soft scaffolds or hyrdogels will be subject to distortion. No guidance can be provided regarding the minimum level of scaffold stiffness required to minimize this source of error.

7.4.2 The pressure required for overcoming porous structure/fluid interactions to induce bubble formation will be

influenced by the surface tension of the wetting fluid, surface energy of the porous material, and adsorbed or absorbed liquids or gases, the rugosity (roughness) of the pore surface and the pore diameter. Capillarity will become increasingly significant with decreasing pore diameter. No guidance is currently available concerning this source of error or regarding minimum detectable pore diameter or susceptibility of scaffolds to artifactual distortion while under testing pressures.

7.5 *Nuclear Magnetic Resonance*—Fluids confined in porous materials behave differently to bulk material, a fact that can be exploited to obtain structural information from NMR. In principle both the longitudinal, t_1 and t_2 relaxation times of hydrogen nuclei within a fluid, such as water, will decrease with decreasing pore diameters. The mean pore diameter and the distribution of pore sizes can be inferred from the spectrum of relaxation times from a porous material. This relatively new technique, referred to as relaxometry (Prado et al (**18**)), can be used to investigate pore dimensions over the nanoscale range.

7.5.1 A complementary method is based on the observation that the melting point of a nanostructured liquid contained within a pore is reduced by an amount that is inversely proportional to its diameter. This decrease in the melting point of the liquid is attributed to a reduction in the size of crystals contained within the pore and the large surface-to-volume ratio. The reduction in melting point is defined by the so-called Gibbs-Thompson function:

$$Tm = k/a \quad (2)$$

where:

Tm = temperature at which melting occurs,
a = typical pore size, and
k = constant.

7.5.2 This method is refered to as cryoporometry. NMR can be used to monitor crystal melting at sub-zero temperatures. From these data the mean pore size and the pore size distribution can be obtained for bulk samples (Strange et al, (**19**, **20**)) or as a function of three-dimensional position in samples located on motorized stages. Cryoporometry can detect pore diameters ranging from a few nanometres to approximately 1 mm. It is a nondestructive method that does not require the use of stains or dyes that has been used to investigate, for example, the structure of clays, porous cements, and sandstones (Song (**21**)).

8. Evaluation of Performance

8.1 Measures of the distribution of pore sizes in the nanoscale range can be obtained from calorimetric and spectroscopic data. The diffusion of molecular probes can be used to investigate larger pore dimensions up to the millimetre length scale.

8.2 *Diffusivity of Markers*—Molecular probes can be used to assess the permeability of scaffolds, especially those based on hydrogels. These probes can range from small molecules (molecular weight range below 1 kDa) to macromolecules such as proteins that have a typical molecular weight range of about 10 to 200 kDa.

8.2.1 Passive diffusion through the matrix can be monitored using simple diffusion cells or the probes can be driven through the matrix by applying a potential difference across it—gel electrophoresis. In principle, molecular diffusivity can be used as a quality control tool to assess the repeatability of manufacturing processes or to investigate the influence of surface charge on permeability. There are practical problems in measuring molecular diffusion in materials that have large pores approaching a millimetre in size, that increase with decreasing path length. The passive diffusion rate in sample geometries that have short path lengths is easily distorted by stirring the fluid on either side of the sample to maintain homogenous concentrations of the probe molecule. The act of removing aliquots, by introducing a transient pressure gradient and or a transient flow, can also affect the rate of molecular diffusion in samples that present virtually no barrier to diffusion. Increasing the path length through changes in geometry can reduce these practical issues.

9. Keywords

9.1 microstructure; pore size; pore volume; porosity; porous materials; tissue scaffolds

APPENDIXES

(Nonmandatory Information)

X1. PERFORMANCE REQUIREMENTS OF TISSUE SCAFFOLDS

X1.1 The success and development of commercial tissue-engineered medical products (TEMPs) in part depends on the establishment of robust manufacturing practices that guarantee that the microstructure of different batches of scaffold constructs is repeatable to within an acceptable tolerance. This requirement stems not only from a need to ensure that cells introduced into the scaffold flourish but also that the scaffold, if it is degradable, is able to maintain its mechanical integrity for a specific period of time until the nascent tissue is able to accommodate this function. The ability to reliably and repeatedly manufacture porous structures will enhance the predictability and consistency of *in vivo* degradation behaviour.

X1.1.1 *The Essential Properties of Tissue Scaffolds*—The primary purpose of tissue scaffolds is to provide a housing for cells or biomolecules that may or may not be absorbable *in vivo*. The materials used to construct the scaffolds can be metals, ceramics, polymers, and composites; of these the highly hydrated soft polymer-based scaffolds are the most challenging structures to characterize. Tissue scaffolds that are intended to accommodate a growing cell culture need to

provide surface conditions that encourage cell adhesion and a distribution of interconnected pores that are large enough to accommodate the cells and enable them to permeate the structure. In addition, the culture conditions within the scaffold need to be able to provide sufficient oxygen for the growing cells and a plentiful supply of nutrients to avoid hypoxia, to sustain a growing population of cells, maintain a stable pH and remove waste products. In part, this is achieved by careful selection of the culture medium and conditions, that is, appropriate mechanical stimulation of the construct during *in vitro* culture that assists natural diffusion of substances into and out of it. However the porosity, pore size distribution, and interconnectivity of pores (tortuosity) play a key role in the efficacy of diffusion processes. Lack of oxygen is a key issue in developing functional TEMPs. Most cells, except tumourous cell lines, experience hypoxia when separated from a supply of oxygen by more than approximately 100 μm **(19)**. This has led to the development of porous walled porous scaffolds that are designed to reduce the diffusion path for oxygen. This approach needs to be followed with caution since it can potentially limit the mechanical integrity of the scaffold and adversely affect its degradation behaviour.

X2. PORE SIZE CLASSIFICATION

X2.1 *Background*:

X2.1.1 The classification of pore sizes, such as those given in Table 2, has yet to be standardized, with definitions of terms varying widely (as much as three orders of magnitude) between differing applications. In many industries, pore size is scaled at a chemical level, commonly referring to the sub-micrometer scale (that is, nanometer) dimensions found within the permeable filtration media involved with gas separation. Accordingly, the IUPAC (International Union of Pure and Applied Chemistry) developed relevant scaling and nomenclature to suit such chemical scale applications, with "micropores" defined as smaller than 2 nm, "mesopores" as between 2 and 50 nm, and "macropores" as larger than 50 nm (>0.05 μm) **(22)**.

X2.1.2 In contrast, descriptions of "microporous" films or foams for use in filtration or surgical dressings applications have since the 1960s described "micropores" as being in the range between 0.1 to 200 μm and have defined the size of "macropores" to be as high as between 200 and 2000 μm (see U.S. Pat. No. 3,281,511 (Goldsmith et al.) issued Oct. 25, 1966; U.S. Pat. No. 3,376,238 (Gregorian et al.), issued Apr. 2, 1968; U.S. Pat. No. 3,870,593 (Elton, et al.), issued March 11, 1975; U.S. Pat. No. 3,931,756 (Van Brunt), issued Jan 13, 1976; and U.S. Pat. No. 3,978,855 (McRae, et al.), issued September 7, 1976.

X2.1.3 These latter definitions and size ranges reasonably approximate the current nomenclature utilized in both particulate and biological filtration applications (see General Electric Osmonics "Microporous Membranes" web site at http://osmolabstore.com/page1022.htm and other references/citations). Despite this historically established and current usage, no standardized terminology has yet been developed for these applications, which emphasize filtration for removal of bacteria (approximately 0.5 μm) or particles, or both. Since porous implant and tissue-engineering applications are both focused primarily on the separation and/or support of mammalian cells (typically 5+ μm), the biological and filtration oriented usage and definitions carry significantly greater relevance to these applications than would the IUPAC scaling system with an upper limit of 50 nm (0.05 μm).

X2.1.4 Perret, et al. **(3)** provides both a discussion and a table that provides an overview of the extensive nomenclature discrepancies and conflicting definitions that exist within the literature. Such discrepancies underscore the need for the generation of standard terminology to facilitate utilization of more consistent language within the scientific community.

X2.2 *Definitions for Life Science Applications*:

X2.2.1 Life Science applications typically consider nanoscale to be 100 nanometers (0.1 μm) or smaller, a definition that is consistent with other fields such as applied physics, materials science, interface and colloid science, device physics, supramolecular chemistry (which refers to the area of chemistry that focuses on the noncovalent bonding interactions of molecules), self-replicating machines and robotics, chemical engineering, mechanical engineering, biological engineering, and electrical engineering.

X2.2.2 In the context of filtration through a porous media, life science applications tend to utilize the term nanoporosity with respect to the filtration of biomolecules or viruses. As discussed in subsection 3.1 (Definitions), microporosity is commonly utilized with respect to the filtration of bacteria, mammalian cells, and tissue. Within the life sciences, the terms microcapillaries, capillaries, and macrocapillaries are not routinely utilized to describe pore size due to the high potential for the terms to be confused with the blood vessels that bridge between arteries and veins.

X2.2.3 Porosity-related definitions suitable for use within a life science context are provided in Section 3, Terminology. In that any of these definitions can shift dependent on the utilized pore size determination technique (see Table 1 and Fig. 1), an accompanying statement describing the utilized measurement technique is essential.

REFERENCES

(1) Tomlins, P.E., Grant, P., Vadgama, P., James, S. Mikhalovsky, S., "Structural Characterisation of Polymer-Based Tissue Scaffolds," National Physical Laboratory, United Kingdom, Measurement Note DEPC-MN-002, May 2004.

(2) Meyer, K., Lorenz, P., Bohl-kuhn, B. and Klobes, P., "Porous Solids and Their Characterisation," *Cryst. Res. Tech.*, Vol. 29(7), 1994, 903–930.

(3) Perret, P., Prasher, S.O., Kantzas, A. and Langford, C., "Three-Dimensional Quantification of Macropore Networks in Undisturbed Soil Cores," *Soil Sci. Soc. Am.*, 63, 1999, p. 1530.

(4) Tjia, J. and Moghe, P., "Analysis of 3-D Microstructure of Porous Poly(lactide-glycolide) Matrices using Confocal Microscopy," *J. Biomed. Mat. Res.*, Vol. 43, No. 3, 1998, pp. 291–299.

(5) Birla, R. and Matthew, H. W. T., "3-Dimensional Imaging & Analysis of Smooth Muscle Colonization of Porous Chitosan Scaffolds," Proc. 1st Joint BMES/EMBS Conf., 1999, p. 119.

(6) *The Handbook of Optical Coherence Tomography*, edited by Bouma and Tearney, Marcel Dekker, Inc., 2002.

(7) Hee, M., Izatt, J., Swanson, E., Huang, D., Schuman, J., lin, C., Puliafito, C. and Fujimoto, J.G., "Optical Coherence Tomography of the Human Retina," *Archives of Opthalmology*, 113, 1995, p. 325.

(8) Barton, J., Milner, T., Pfefer, T., Nelson, J. and Welch, A. "Optical Low Coherence Reflectometry to Enhance Monte Carlo Modeling of Skin," *J. of Biomed. Opt.* 2(2), 1997, p. 226.

(9) Boppart, S., Brezinski, M., Bouma, B., Tearney G. and Fujimoto, "Investigation of Developing Embryonic Morphology Using Optical Coherence Tomography," *J. Developmental Biology* 177, 1996, p.54.

(10) McDonough, W.G., Amis, E. J., Kohn, J., "Critical Issues in the Characterization of Polymers for Medical Applications", NISTIR-6535 (NIST, Gaithersburg, MD, 2000).

(11) Dunkers, J., Cicerone, M. and Washburn, N., "Collinear Optical Coherence and Confocal Fluorescence Microscopies for Tissue Engineering," *Optics Express*, 2003.

(12) Müller, R., Hahn, M., Vogel, M., Delling, G. and Rüegsegger P., "Morphometric Analysis of Noninvasively Assessed Bone Biopsies: Comparison of High-Resolution Computed Tomography and Histologic Sections," *Bone*, 18, 1996, pp. 215–220.

(13) Müller, R., Matter, S., Neuenschwander, P., Suter, U.W. and Rüegsegger P., "3-D Micro-Tomographic Imaging and Quantitative Morphometry for the Nondestructive Evaluation of Porous Biomaterials," In R. M. Briber, D. G. Pfeiffer, C. C. Han, editors, Morphological Control in Multiphase Polymer Mixtures, *Mat. Res. Soc.*, Vol. 461, 1997, pp. 217–222.

(14) Van Oosterwijck, H., Duyck, J., Vander Sloten, J., Van Der Perre, G., Jansen, J., Wevers M. and Naert, I., "The Use of Microfocus Computerized Tomography as a New Technique to Characterize Bone Tissue Around Oral Implants," *Journal of Oral Implantology*, 26, 2000, pp. 5–12.

(15) Maspero, F. A., Ruffieux, K., Muller, B., Wintermantel, E., "Resorbable Defect Analog PLGA Scaffolds using CO2 as Solvent: Structural Characterization," *J Biomed Mater Res.,* Oct; 62(1), 2002, pp.89–98.

(16) Lin, A. S., Barrows, T.H., Cartmell, S. H., Guldberg, R. E., "Microarchitectural and Mechanical Characterization of Oriented Porous Polymer Scaffolds," *Biomaterials*, Feb;24(3), 2003, pp. 481–489.

(17) Scaglione, S., Beltrame, F., Diaspro, A., Usai, C. and Mastrogiacomo, M., "Tissue Engineering: Methods for Bone Quantification and Scaffolds Geometric Properties Analysis," *Proc. Focus on Microscopy 2003*, 2003.

(18) Prado, P.J., Balcom, B.J., Beyea, S.D., Bremner, T.W., Armstrong, R.L., Pishe, R. and Gratten-Bellew, P.E., "Spatially Resolved Relaxometry and Pore Size Distribution by Single-Point NMR Methods: Porous Media Calorimetry," *J. Phys. D: Appl. Phys.*, 31, 1998, pp. 2040–2050.

(19) Strange, J.H., Webber, J.B., Schmidt, S.D., "Pore Size Distribution Mapping," *Magn Reson Imaging*, 14(7-8), 1996, pp. 803–805.

(20) Strange, J.H., Rahman, M. and Smith E.G., "Characterisation of Porous Solids by NMR," *Physical Review Letters*, 71, No. 21, 1993, pp. 3589–3591.

(21) Song Y.Q., "Pore Sizes and Pore Connectivity in Rocks Using the Effect of Internal Field," *Magn Reson Imaging.*, 19(3-4), 2001, pp. 417–421.

(22) *Pure & Appl. Chem*, Vol 66, No. 8, 1994, pp. 1739–1758.